Theory of multiple proton-electron transfer reactions and its implications for electrocatalysis

Marc T.M. Koper[a,b]

[a)]*Leiden Institute of Chemistry, Leiden University, PO Box 9502, 2300 RA Leiden, The Netherlands;* [b)]*Catalysis Research Center, Hokkaido University, Sapporo 001-0021, Hokkaido, Japan*

E-mail: m.koper@chem.leidenuniv.nl

Abstract

This Perspective article outlines a simple but general theoretical analysis for multiple proton-electron transfer reactions, based on the microscopic theory of proton-coupled electron transfer reactions, recent developments in the thermodynamic theory of multi-step electron transfer reactions, and the experimental realization that many multiple proton-coupled electron transfer reactions feature decoupled proton-electron steps in their mechanism. It is shown that decoupling of proton and electron transfer leads to a strong pH dependence of the overall catalytic reaction, implying an optimal pH for high catalytic turnover, and an associated optimal catalyst at the optimal pH. When more than one catalytic intermediate is involved, scaling relationships between intermediates may dictate the optimal catalyst and limit the extent of reversibility that may be achievable for a multiple proton-electron-transfer reaction. The theory is discussed in relation to the experimental results for a number of redox reactions that are of importance for sustainable energy conversion, primarily focusing on their pH dependence.

1. Introduction

The vast majority of redox reactions that is currently studied for fuel cells[1] and for the (photo-)electrochemical production of fuels[2,3] involve the simultaneous transfer of an equal number of electrons and protons:

$$A + n\,H^+ + n\,e^- \leftrightarrows B \qquad (1)$$

[or the equivalent "alkaline version": A + n H_2O + n e^- ⇆ B + n OH^-]. Reaction (1) includes the hydrogen oxidation reaction (HOR), the hydrogen evolution reaction (HER), the oxygen reduction reaction (ORR), the oxygen evolution reaction (OER), the reduction of carbon dioxide to a variety of small organic molecules, as well as the reverse oxidation of small organic molecules. The development of efficient catalysts for these multiple proton-electron transfer reactions is of key importance for the development of a sustainable energy cycle.

Remarkably, standard electrochemistry textbook theories of electrode reactions offer little to no insight into how to develop such catalysts. Theories such as the empirical Butler-Volmer theory[4] and the more molecular-level Marcus theory[4,5] focus primarily on the role of the electrode potential and the role of the solvent (in the case of the Marcus theory), but the role of the metal catalyst is essentially reduced to that of an electron donor or acceptor with an infinite number of closely spaced energy levels.

To understand the role of the catalyst, we must account for a strong interaction between the catalyst and the intermediates of the reaction. An extremely useful principle from heterogeneous catalysis, the so-called Sabatier principle,[6,7] states that the best catalyst binds the key intermediate(s) neither too weakly nor too strongly. In the former case, the catalyst is unable to activate the reactant, in the latter case the catalyst will be become poisoned by strongly adsorbed intermediates. A quantitative formulation of the Sabatier principle can be based on the thermodynamics of the separate reaction steps, where the free energy of reaction steps involving catalyst-bound intermediates will depend on the nature of the catalyst. In the quantitative formulation of the Sabatier principle, the best catalyst is that substance for which each reaction step in the sequence of steps is thermodynamically neutral or downhill. Under conditions of electrochemical equilibrium, this implies that each step in a reaction mechanism must have an equilibrium potential equal to the overall equilibrium potential, and if the mechanism contains non-electrochemical steps, such steps must have zero free reaction energy. If such a condition is or can not be satisfied, the thermodynamic Sabatier approach identifies the "difficult" step in the mechanism as that step that is thermodynamically least favorable. This step is

often but certainly not always the same as the rate-determining step, and I will come back to this subtle but important distinction later on in this Perspective.

The Sabatier approach has been revived in the last 10 years by the extensive work of the group of Nørskov,[8] who has combined it with quantum-chemical calculations (based on Density Functional Theory DFT) of the thermodynamics of the reaction steps in a catalytic mechanism. This approach allows for the "computational screening" of a large number of catalysts and has proven very useful in the rational development of new catalysts. The approach has also become very popular in electrocatalysis, and has been applied to all of the above-mentioned electrode reactions.[9,10,11,12,13,14]

However, the thermodynamic approach has also revealed important limitations of multi-step catalytic reactions involving more than one intermediate, namely that the intermediates in a catalytic reaction have energetic relationships with each other, called scaling relationships.[11,15] These scaling relationships find their origin in the quantum-chemical theory of chemical bonding.[16,17,18] The scaling relationships lead to the situation that the optimal catalyst as defined above (i.e. all reaction steps being thermodynamically neutral) cannot be reached, because of the unfavorable universal scaling relation between the energies of two (or more) intermediates. For the ORR and the OER, this unfavorable scaling was found to exist between the OOH and the OH intermediates.[19,20] The energy difference between these two intermediates is always ca. 3.2 ± 0.2 eV; this energy difference exists when the two species do not interact with a catalyst, and stays in tact on any (two-dimensional) surface to which they bind, because they coordinate to the surface in an identical way. However, for an ideal catalyst, the energy difference should be 2.46 eV (i.e. 2 x 1.23 eV; 1.23 V being the standard equilibrium potential of the ORR/OER). As a result, there is a "fundamental" overpotential for both ORR and OER of (3.2±0.2 - 2.46 eV)/2e ≈ 0.25 - 0.35 V. A similar universal scaling between the CO and HCO intermediates was also argued to limit the reversibility of the electrocatalytic CO_2 reduction.[13]

The universal scaling between two catalytic intermediates, which was first realized in ref.19, and later confirmed in detail for a number of different catalyst surfaces,[20,21,22,23] has profoundly influenced my thinking about the catalysis of multi-electron transfer reactions. If the idea of scaling is correct, we must devise strategies to overcome it. One

possible strategy is to develop catalysts that can bind the two intermediates in different ways, for instance by building a three-dimensional active site (see, e.g., ref.13). This strategy should (de)stabilize one intermediate, without affecting the other, and it was recently argued on the basis of theoretical calculations that enzymes for the interconversion of CO_2 and CO "use" this strategy.[24]

An alternative strategy is to find pathways in which one of the intermediates is avoided. The main topic of this Perspective is a precipitate of that second strategy, and is related to another interesting but related issue of redox catalysis that developed from a comparison of the mechanisms of the ORR and OER on heterogeneous electrocatalysts and redox enzymes.[25] In heterogeneous electrocatalysis it is typically assumed that the proton(s) and the electron(s) in Eq.1 transfer simultaneously at each step in the mechanism, and this assumption is also made in arriving at the idea of the scaling relations. However, such mechanisms are rather untypical for redox enzymes. Because of the localized nature of the transferred charge in redox enzymes, the decoupling of proton and electron transfer appears to be much more common place. Such a decoupling will involve intermediates that do not feature in the mechanisms suggested for heterogeneous catalysts. As a result of the decoupling of proton and electron transfer, the pH of the reactive medium plays a very active role in the catalysis, whereas pH plays essentially no role in the existing thermodynamic theories of electrocatalysis. As I will argue further on in this Perspective, such an under-appreciation of the role of pH in theory is unwarranted, as practically all reactions mentioned above are known to be pH dependent, also in heterogeneous electrocatalysis.

The aim of this Perspective article is to outline the thermodynamic theory of multiple proton-electron transfer reactions, incorporating the possibility of pathways involving the decoupling of proton and electron transfer, as such pathways are neglected in the current thermodynamic theories of electrocatalysis.[10,12,13,19] Since the conditions for the decoupling of proton and electron transfer follow from the microscopic theory of proton-coupled electron transfer reactions, I will first briefly summarize the pertinent results from the Marcus-type theories that have been developed for the one proton-electron transfer reactions (i.e. n=1 in Eq.1) in Section 2. This theory basically equips us with approximate expressions for the activation energies of the separate steps to be considered

in the more elaborate mechanisms for proton and electron transfer reactions involving more than one electron (i.e. $n \geq 2$ in Eq.1). Similar to a previous paper,[19] I will consider the n=2 (Section 3) and n=4 (Section 4) separately, treating the ORR as a generic n=4 reaction and applying the insights of Sections 2 and 3 to organize some of the experimental data on this reaction. A further brief comparison to other reactions will be given in Section 5. The paper closes with a summary of conclusions in Section 6.

2. Single proton-coupled electron transfer (1-PCET)

In this section, I will summarize some of the main model concepts, activation energies and rate expressions for a single proton-coupled electron transfer reaction.[26,27,28,29,30,31,32,33] We will consider a redox reaction studied in an electrochemical cell but much of what follows can also be applied to a non-electrochemical proton-coupled transfer reaction. The reasons for focusing on the electrochemical case are related to the importance of (multiple) proton-coupled electron transfer in electrochemical devices, as referred to in the Introduction, and to the convenience with which the thermodynamic driving force can be defined and applied in an electrochemical cell.

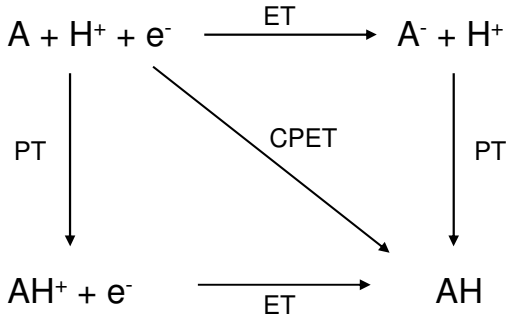

Figure 1. Square scheme for proton-coupled electron transfer. ET=electron transfer, PT=proton transfer, CPET=concerted proton-electron transfer.

The redox reaction of interest is written as:

$$A + H^+ + e^- \leftrightarrows AH \tag{2}$$

and its sequential and concerted pathways are drawn in the familiar square scheme of Figure 1. Reaction 2 has a standard equilibrium potential given by:

$$E^0_{A,H^+/AH} = -\frac{G(AH) - G(A) - G(H^+)}{e_0} \tag{3}$$

where the G's are free energies of formation and e_0 is the unit of charge. The rates of the various pathways illustrated in Figure 1 are determined by the free energies of the "off-diagonal" states A^- and AH^+, by the reorganization energies of the solvent and other local reactive modes as they couple to the electron transfer (λ_{ET}) and the proton transfer (λ_{PT}), as well as by a cross coupling reorganization energy ($\bar{\lambda}$), and by pre-exponential rate constants which may reflect effects of solvent dynamics, electronic adiabaticity and proton tunneling.[32] Figure 2 shows a typical potential energy surface spanned by the collective solvent coordinate coupled to electron transfer (ET) and the collective solvent coordinate coupled to proton transfer (PT). At the equilibrium potential of reaction 2, the free energy of the A^- state with the respect to the initial or final state is given by:

$$G(A^-) = -EA(A) + \Delta G_{solv}(A^-) \tag{4}$$

with EA(A) the electron affinity of A and $\Delta G_{solv}(A^-)$ the solvation energy of A^-. The free energy of the AH^+ state with respect to the initial or final state is given by:

$$G(AH^+) = \Delta G_{prot}(A) - G(H^+) \tag{5}$$

with $\Delta G_{prot}(A)$ the protonation energy of A. The free energy of the proton $G(H^+)$ is defined as zero at pH=0 (standard conditions), and equals $G(H^+)$ = -2.303*RT*pH at all other pHs.

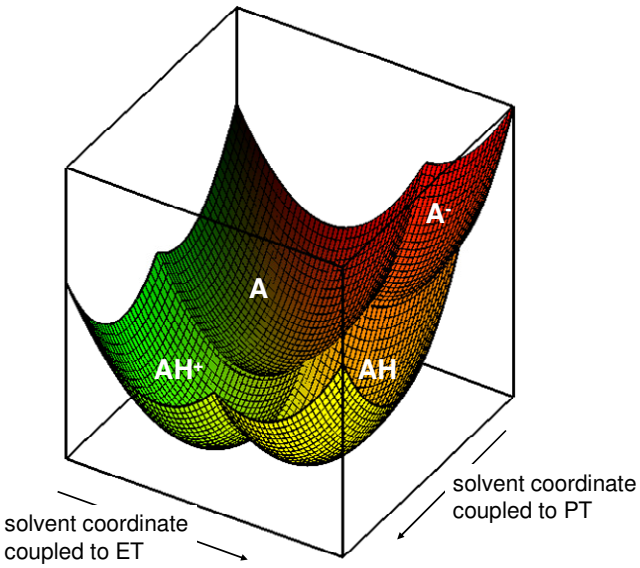

Figure 2. Typical two-dimensional potential energy surface for reaction 2. The four regions corresponding to the four states of Figure 1 can be clearly recognized. Whether a minimum in potential energy develops in the two "off-diagonal" regions corresponding to the AH^+ and A^- states depends on their equilibrium energies given by Eqs.4 and 5.

The ET-coupled solvent reorganization energy λ_{ET} may be estimated by the classical Marcus expression:[5]

$$\lambda_{ET} = \frac{e_0^2}{4\pi\varepsilon_0}\left(\frac{1}{\varepsilon_{opt}} - \frac{1}{\varepsilon_s}\right)\frac{1}{2a} \qquad (6)$$

where ε_0 is the vacuum permittivity, ε_{opt} is the optical dielectric constant of the solvent, ε_s is the static dielectric constant of the solvent, and a is the radius of A and A^-. Note that the linear response approximation of the Marcus theory assumes that the radii of A and A^- are the same. This is a rather strong assumption and we have shown previously by molecular dynamics simulations that the nonlinearity of the solvent response is especially severe in the transition from charge 0 to -1 due to significant changes in electrostriction.[34]

The PT-coupled solvent reorganization λ_{PT} may be estimated as the dielectrically slow part of the Kirkwood-Onsager expression[35,36] for the solvation energy of a dipole μ:[30]

$$\lambda_{PT} = \frac{1}{4\pi\varepsilon_0}\left(\frac{\varepsilon_s - 1}{2\varepsilon_s + 1} - \frac{\varepsilon_{opt} - 1}{2\varepsilon_{opt} + 1}\right)\frac{\mu}{a^3} \qquad (7)$$

where a is the radius of the spherical cavity containing the dipole. If we consider a as the distance of closest approach between H^+ and A^- in their dissociated state, $\mu \approx e_0 a$. The radius a would roughly correspond to the distance between H^+ and A^- in the prereactant state of the Eigen-Weller model for proton transfer.[37,38] It is noteworthy that λ_{PT} is typically smaller than λ_{ET}[30] as proton transfer is related to the creation or annihilation of a dipole, which is energetically less costly than the creation or annihilation of an ion.

The cross-coupling reorganization energy $\bar{\lambda}$ expresses the extent of overlap or coupling between the electron-coupled and proton-coupled solvent modes.[27,28,29,33] If we consider the usual linear response model for the electrostatic solvent coupling, it is easy to see that the cross-coupling reorganization energy must be 0 if electron and proton transfer are directionally orthogonal (see Fig.3a), as this implies absence of reorganizational overlap. There are no model expressions available for $\bar{\lambda}$ but if we assume that for a hydrogen atom transfer (HAT) reaction (Fig.3b), the electrostatic contribution of the solvent reorganization is zero[39] (since effectively no charge is transferred), from the expression for the concerted proton-electron transfer (CPET) reorganization energy:[27,28,33]

$$\lambda_{CPET} = \lambda_{ET} + \lambda_{PT} + 2\bar{\lambda} \qquad (8)$$

it follows that $\bar{\lambda}_{HAT} = -(\lambda_{ET} + \lambda_{PT})/2$, i.e. there is full solvent overlap. In a truly linear response model, the overlap for directionally opposite proton-electron transfer (Fig.3c) must consequently be $\bar{\lambda} = (\lambda_{ET} + \lambda_{PT})/2$, by symmetry. For intermediate situations, a simple expression for the value for $\bar{\lambda}$ would follow from a projection of the angle θ between the direction of proton and electron transfer, i.e. $\bar{\lambda} = -(\lambda_{ET} + \lambda_{PT})\cos\theta/2$ (see Fig.3a). Hammes-Schiffer et al. have carried out simulations of orthogonal and collinear proton-electron transfer in solution (not at an electrode), such as depicted in Fig.3a and

3b, and calculated $\bar{\lambda}$ for both cases from a dielectric continuum model.[40,41] For the situation shown in Fig.3b, $\bar{\lambda}$ was indeed found to be quite large and negative, but it did not entirely cancel the $\lambda_{ET} + \lambda_{PT}$ term in Eq.8. In their model, this must be due to the fact that the proton and the electron were not centered on the same sites on the donor and acceptor species, so that effectively a dipole was transferred. Note that such a situation would also apply to Figure 3b, as it effectively involves the annihilation of a dipole consisting of the proton in solution and its image charge in the electrode. Nevertheless, a situation such as illustrated in Fig.3b leads a lower overall λ_{CPET} than the sum of λ_{ET} and λ_{PT} since this situation requires a smaller change in charge distribution.[41] Of course, the cartoon shown in Figure 3 is oversimplified and does not include any internal reorganization within A, but it does illustrate the importance of directionality in proton-coupled electron transfer.

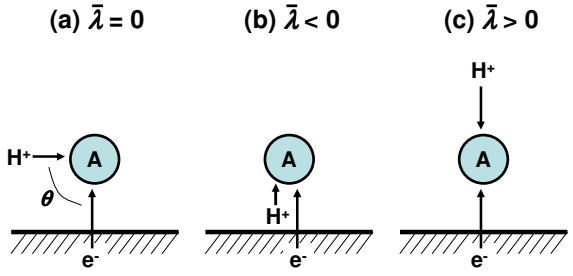

Figure 3. Directionality of the proton and electron transfer determines the extent of solvent overlap $\bar{\lambda}$, or cross reorganization energy.

The activation energies for the ET, PT, and concerted proton-electron transfer (CPET) are given by the usual Marcus formula:

$$\Delta G_i^{act} = \frac{\left(\lambda_i + \Delta G_i^0\right)^2}{4\lambda_i} \qquad (9)$$

where i = ET, PT or CPET, and ΔG_i^0 is the free reaction energy of the corresponding reaction. These free energies of activation can be used in combination with the usual Transition-State-Theory expression for the reaction rate. The pre-exponential factors for the rates of the various reactions have many different expressions, depending on the exact conditions of the reaction dynamics. It is not the purpose of this article to summarize this more technical part of the theory of proton-coupled electron transfer. Hammes-Schiffer and Stuchebrukhov[32] have reviewed extensively the role of proton tunneling, electronic adiabaticity and solvent dynamics on the pre-exponential factor, and we refer the interested reader to that paper.

From the above equations, we can derive the conditions for decoupled vs. concerted proton-electron transfer for single proton-coupled electron transfer reaction in the presence of an applied overpotential η/e_0. For a reduction reaction, proton-electron transfer will decouple if one of their activation energies is smaller than the activation for CPET:

$$\frac{\left[\lambda_{\mathrm{ET}} + G(\mathrm{A}^-) + \eta\right]^2}{4\lambda_{\mathrm{ET}}}, \frac{\left[\lambda_{\mathrm{PT}} + G(\mathrm{AH}^+)\right]^2}{4\lambda_{\mathrm{PT}}} < \frac{\left[\lambda_{\mathrm{CPET}} + G(\mathrm{AH}) + \eta\right]^2}{4\lambda_{\mathrm{CPET}}} \qquad (10)$$

(where we have set the energy of A + H^+ equal to zero). In words: if the proton or electron affinity of A is sufficiently favorable, proton and electron transfer will decouple. For an oxidation reaction, decoupled ET or PT will be preferred if:

$$\frac{\left[\lambda_{\mathrm{PT}} + G(\mathrm{A}^-) - G(\mathrm{AH})\right]^2}{4\lambda_{\mathrm{PT}}}, \frac{\left[\lambda_{\mathrm{ET}} + G(\mathrm{AH}^+) - G(\mathrm{AH}) - \eta\right]^2}{4\lambda_{\mathrm{ET}}} < \frac{\left[\lambda_{\mathrm{CPET}} - G(\mathrm{AH}) - \eta\right]^2}{4\lambda_{\mathrm{CPET}}} \qquad (11)$$

In words: if there is a high tendency for a proton or an electron to leave AH, proton and electron transfer will decouple. Note that if $\bar{\lambda}$ is not very negative, ET or PT are always favored over CPET if either one of them is thermodynamically equivalent to CPET, due to their lower activation barrier. Typically, many PCET reactions favor CPET pathways as a way to avoid the high-energy intermediates associated with the ET and PT pathways, and therefore the reason for concerted proton-electron transfer is often thermodynamic.

Hammes-Schiffer et al. have studied a number of examples of CPET reactions by molecular simulations.[42,43,44] Of course, such statements do not account for the role of the pre-exponential factor, proton tunneling, electronic adiabaticity, or solvent dynamics. Conditions very similar to Eq.10 and 11 have been formulated by Costentin et al.[45]

We also note that in above equations catalysis does not play a clear role. One may consider catalytic effects to be incorporated in the energy of the various states, if the energy of interaction of the state with the catalyst is accounted for. However, the expression for the activation energy includes only the reorganization of the solvent and the surrounding medium. No catalysis is involved. It is possible to incorporate explicitly the role of the metal catalyst, but no analytical expressions for the activation energy have been derived.[46]

3. Two proton-coupled electron transfer (2-PCET)

In the case of a two-proton two-electron transfer reaction, i.e.

$$A + 2H^+ + 2e^- \leftrightarrows AH_2 \tag{12}$$

the general square scheme is given in Figure 4. This reaction has a standard equilibrium potential given by:

$$E^0_{A,\,2H^+/AH_2} = -\frac{G(AH_2) - G(A) - 2G(H^+)}{2e_0} \tag{13}$$

where as before the G's are the free energies of formation of the different species, and e_0 is the unit of charge. In this scheme, it is assumed that A and AH_2 are species in solution, whereas all other intermediates can be either in solution or bound to a catalyst. For instance, the hydrogen evolution/oxidation reaction would correspond to the case where "A" represents the catalyst, AH represents the hydrogen bound to the catalyst, and the A-H_2 bond strength is zero. As another example, for the formic acid/carbon dioxide redox

couple, A represents CO_2, AH (surface-adsorbed) formate, and AH^- the formate anion (adsorbed or in solution).

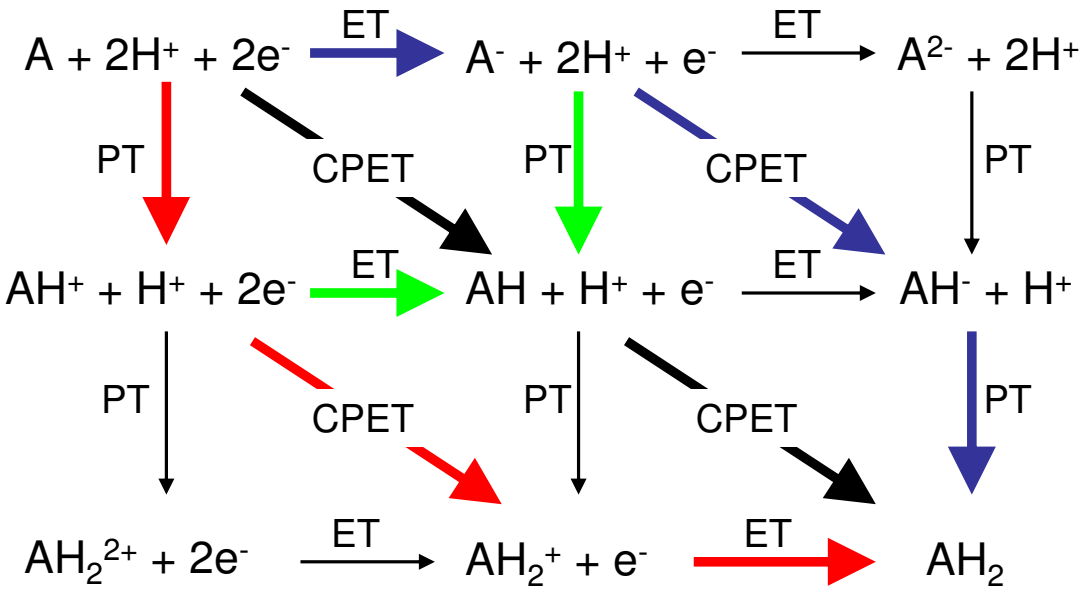

Figure 4. Square scheme for a two-proton two-electron transfer reaction, Eq.12. Black pathway is the fully concerted pathway. Red pathway is the "protonation" pathway. Blue pathway is the "electronation" pathway. In a pathway following one of the green lines, the first PCET is sequential, the second PCET is concerted.

Rather than focusing on the rate expressions for the separate elementary steps in Figure 4, which have been discussed in Section 2, this Section will consider a thermodynamic analysis of four different pathways through the scheme shown in Figure 4. Such an analysis provides the necessary but not sufficient conditions for achieving optimal catalysis. The analysis is based on a quantitative formulation of the Sabatier principle as applied to multi-step catalytic reactions, which states qualitatively that a good catalyst binds the key intermediates neither too weakly nor too strongly. The quantitative formulation of the Sabatier principle is that the optimal catalyst is the one which provides a thermodynamically flat landscape: all steps in the mechanism must be

thermodynamically neutral or downhill.[10,19,47] For a redox reactions such as Eq.1 and 12, this implies that:

For optimal "reversible" electrocatalysis, the equilibrium potentials of all reaction steps must be equal to the overall equilibrium potential, or if non-electrochemical steps are involved, the Gibbs free energy of each reaction step must be zero.

This statement will be our guiding principle in this and in the next section. One must carefully distinguish between this thermodynamic analysis and an analysis based on rate-determining steps, which requires knowledge of the activation barriers and the rate laws of the different steps.[48] The statement is a useful postulate, but not a law. It is not difficult to formulate kinetic models that will not fulfill the above statement (see, e.g., ref.48). This distinction bears a relation to a discussion in the heterogeneous catalysis literature on the analysis of catalytic reaction schemes based on the concept of "degree of rate control", which requires knowledge of activation barriers or rate constants, or on the concept of De Donder affinities, which only require knowledge of the thermodynamics of the separate steps.[49,50,51,52] Although the Sabatier has distinct limitations related to the fact that kinetics is not included, the thermodynamic Sabatier-type analysis is typically accurate in identifying the bottleneck in a mechanism, as has been argued at various places in the literature.[9,19,47,51] There may be fundamental restrictions why such a thermodynamically optimal situation may not be achievable, in which case we are looking for the catalyst with the lowest overpotential, which in our thermodynamic analysis corresponds to the situation where all steps are either thermodynamically neutral or downhill. Such an overpotential is called the "thermodynamic overpotential",[10] which is given the symbol η_T.

Fully concerted pathway. The first pathway, which is the fully concerted pathway typically considered in surface electrochemistry, and which is indicated by the black arrows in Figure 4, consists of two CPET reaction steps:

$$A + H^+ + e^- \leftrightarrows AH \qquad (14a)$$

$$AH + H^+ + e^- \leftrightarrows AH_2 \tag{14b}$$

The analysis of this mechanism is straightforward and has been discussed in detail in the literature. We may define the equilibrium potentials of the two steps as:

$$E^0_{A,H^+/AH} = -\frac{G(AH) - G(A) - G(H^+)}{e_0} \tag{15a}$$

$$E^0_{AH,H^+/AH_2} = -\frac{G(AH_2) - G(AH) - G(H^+)}{e_0} \tag{15b}$$

where we note that

$$E^0_{A,\,2H^+/AH_2} = \frac{1}{2}\left(E^0_{A,\,H^+/AH_2} + E^0_{AH,\,H^+/AH_2}\right) \tag{16}$$

Since all three equilibrium potentials contain the same $G(H^+)/e_0$ term, it is useful to redefine the potentials on the Reversible Hydrogen Electrode (RHE) scale:

$$E_i^{0,RHE} = E_i^0 - \frac{G(H^+)}{e_0} \tag{17}$$

Without loss of generality, we may set the overall equilibrium potential $E^{0,RHE}_{A,\,2H^+/AH_2}$ equal to zero, which implies that $G(AH_2) = G(A)$, so that Eqs.15a and 15b simplify to:

$$E^{0,RHE}_{A,H^+/AH} = -\frac{G(AH) - G(A)}{e_0} \tag{18a}$$

$$E^{0,RHE}_{AH,H^+/AH_2} = -\frac{G(A) - G(AH)}{e_0} \tag{18b}$$

Figure 5 plots these equilibrium potentials as a function of the "descriptor" $G(\mathrm{AH}) - G(\mathrm{A})$, showing that the optimal catalytic situation is obtained when $G(\mathrm{AH}) - G(\mathrm{A}) = 0$. At positive (negative) values of $G(\mathrm{AH}) - G(\mathrm{A})$, reaction 14a (14b) is thermodynamically unfavorable and therefore determines the thermodynamic overpotential η_T of the overall reaction. Such a reaction is termed "potential determining". The optimal catalyst at $G(\mathrm{AH}) - G(\mathrm{A}) = 0$ corresponds to the top of the volcano in the well-known volcano plot of heterogeneous catalysis. This situation has been studied extensively in relation to the electrocatalytic hydrogen evolution reaction and the reader is referred to the literature for detailed discussions[9,19,53,54,55,56,57] as well as for a convincing experimental example of an experimental volcano plot for the hydrogen evolution reaction.[58]

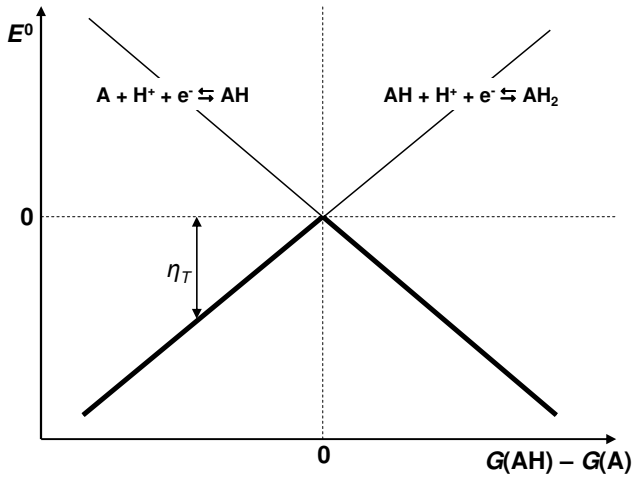

Figure 5. Plot of the equilibrium potentials Eqs.18a and 18b of reactions 14a and 14b as a function of the "descriptor" $G(\mathrm{AH}) - G(\mathrm{A})$. On the positive side of $G(\mathrm{AH}) - G(\mathrm{A}) = 0$, reaction 14a is potential determining; on the negative side, reaction 14b is potential determining. The thick solid lines give the thermodynamic volcano curve for the overall reduction reaction.

Decoupled proton-electron transfer pathways. Here we will consider three alternative pathways to the fully concerted pathway, two of which bypass the formation of the AH intermediate. One pathway goes through the AH^+ and the AH_2^+ intermediates, which may be termed the "protonation" pathway (when considered as a reduction reaction, indicated by the red arrows in Figure 4); the other pathway goes through the A^- and the AH^- intermediates, which may be termed the "electronation" pathway (when considered as a reduction, indicated by the blue arrows in Figure 4). The third pathway forms the AH

intermediate in a sequential PCET reaction rather than a CPET reaction (indicated by the green arrows shortcutting from the red and blue pathways to the black pathway in Figure 4).

The protonation pathway consists of the following three reaction steps:

$$A + H^+ \leftrightarrows AH^+ \tag{19a}$$

$$AH^+ + H^+ + e^- \leftrightarrows AH_2^+ \tag{19b}$$

$$AH_2^+ + e^- \leftrightarrows AH_2 \tag{19c}$$

Since one step in this sequence does not involve electron transfer, we will not write the equilibrium potentials but instead the Gibbs free energies for the three reactions:

$$\Delta G_{A/AH^+} = G(AH^+) - G(A) - G(H^+) = PA(A) - G(H^+) = -2.303RT * \left[pK_a(A) - pH\right] \tag{20a}$$

$$\begin{aligned} \Delta G_{AH^+,H^+/AH_2^+} &= G(AH_2^+) - G(AH^+) - G(H^+) + e_0E \\ &= -\left[EA(AH_2^+) + PA(A)\right] + \Delta G^0 - G(H^+) + e_0E \end{aligned} \tag{20b}$$

$$\Delta G_{AH_2^+/AH_2} = G(AH_2) - G(AH_2^+) + e_0E = EA(AH_2^+) + e_0E \tag{20c}$$

where $\Delta G^0 = G(AH_2) - G(A)$, and where the second equality in Eq.20b follows from the definitions of PA(A) and EA(AH_2^+) given in Eqs.20a and 20c and the definition of ΔG^0. The overall equilibrium potential of the reaction is given by:

$$E^{eq}_{AH_2/2H^+} = -\frac{\Delta G^0 - 2G(H^+)}{2e_0} \tag{21}$$

Without loss of generality, we may choose this potential as our reference and set it equal to zero, so that at thermodynamic equilibrium $\Delta G^0 = 2G(H^+)$. As we study the

reversibility of the reaction at the equilibrium potential, we set $E = 0$ in Eqs.20b and 20c. As a result, Eqs.20a-c simplify to:

$$\Delta G_{A/AH^+} = \Delta G_1 = \mathrm{PA} - G(\mathrm{H}^+) \tag{22a}$$

$$\Delta G_{AH^+,H^+/AH_2^+} = \Delta G_2 = -[\mathrm{EA} + \mathrm{PA}] + G(\mathrm{H}^+) \tag{22b}$$

$$\Delta G_{AH_2^+/AH_2} = \Delta G_3 = \mathrm{EA} \tag{22c}$$

The reaction is now characterized by three thermodynamic parameters: the proton affinity (or pK_a) of A, PA = PA(A), the electron affinity of AH_2^+, EA = EA(AH_2^+), and the pH (or $G(H^+)$).

Figure 6 shows three plots of the Gibbs free reaction energies as a function of EA, for the typical cases that A has a favorable proton affinity at the working pH (i.e. pK_a > pH, Fig.6a), an unfavorable proton affinity at working pH (i.e. pK_a < pH, Fig.6c), and for pK_a = pH (Fig.6b). Figure 6 plots -ΔG as in that case the thermodynamically unfavorable reactions (ΔG>0) are below the zero line, and the lines connecting the ΔG's of the thermodynamically most unfavorable reactions as a function of EA (bold lines in Figure 6) have the shape of a volcano in such a plot. Figure 6 clearly illustrates that only if pK_a = pH (Fig.6b), an optimal catalyst with zero thermodynamic overpotential can be found, as defined by EA = 0. In the two other cases, the reaction will always have a "sub-optimal" catalyst at best. Note that if pK_a > pH, the optimal catalyst is not the same as that for pK_a = pH. Also, the shape of the volcano is different for ΔG_1<0 (Fig.6a) or ΔG_1>0 (Fig.6c), as the latter has a flat top. However, we do note that in the latter case, i.e. ΔG_1>0, decoupled proton-electron transfer becomes less likely (as the proton affinity is low).

Let us analyze the situation for which the pH is not adjusted to the optimal value, which, I would suspect, would be the situation for the majority of electrocatalytic redox reactions studied experimentally in the literature. If pK_a > pH, the (sub)optimal catalyst is at the intersection between ΔG_2 and ΔG_3, having a thermodynamic overpotential equal to:

$$\eta_T = \frac{\Delta G_T}{e_0} = \frac{\mathrm{EA}_T}{e_0} = \frac{-\mathrm{PA} + G(\mathrm{H}^+)}{2e_0} = \frac{2.303RT(\mathrm{p}K_a - \mathrm{pH})}{2F} \tag{23}$$

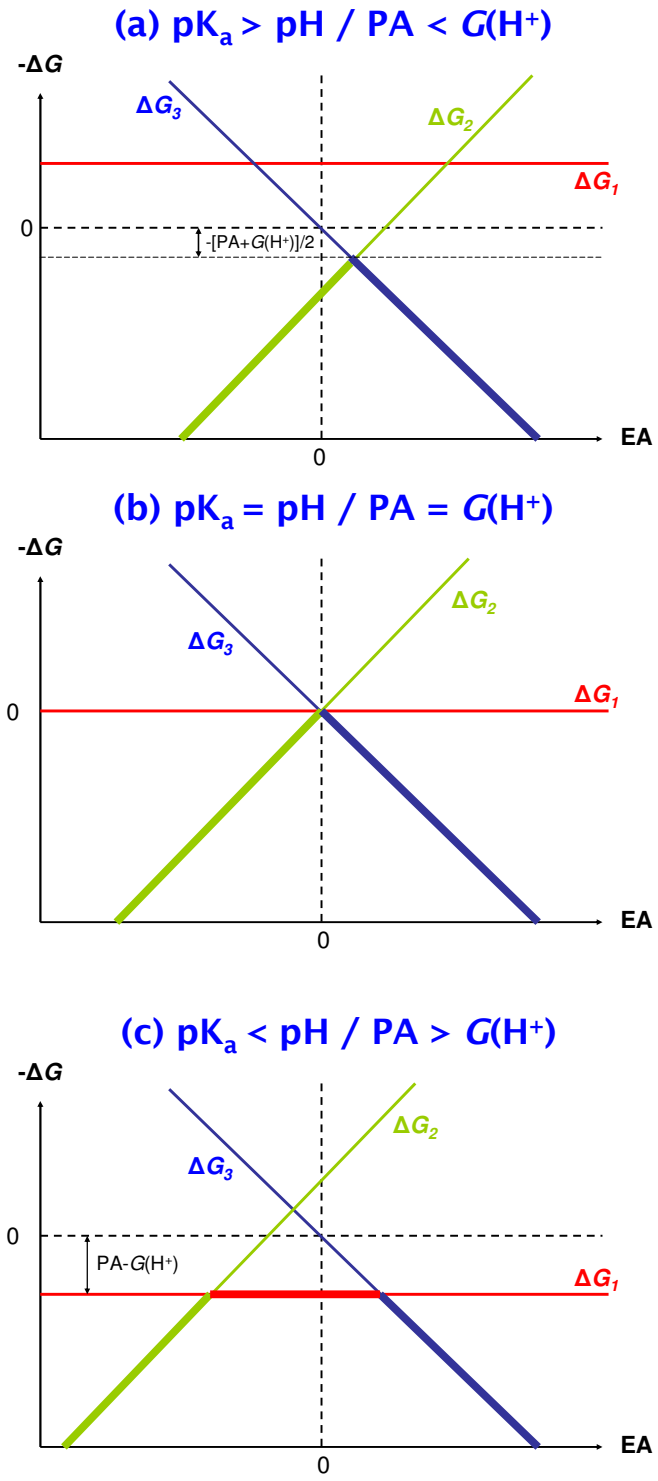

Figure 6. Thermodynamic volcano plots for the reaction mechanism represented by Eqs.17a, 17b and 17c. (a) pK_a > pH, or PA<G(H$^+$); (b) pK_a = pH, or PA=G(H$^+$); (c) pK_a < pH, or PA>G(H$^+$).

showing that the thermodynamic overpotential of the (sub)optimal catalyst is proportional to the deviation of the working pH from the pK_a of the intermediate. As mentioned, if pK_a < pH, the thermodynamic volcano consists of three regions, with a flat region (which should yield a flat-topped volcano). The flat region represents a thermodynamic overpotential equal to -2.303RT(pK_a – pH)/F.

Since the solution pH is an experimentally more accessible quantity than the electron affinity EA, it useful to perform the same analysis, but with the pH as the "descriptor". In this case, we must consider the three situations EA < 0, EA = 0, and EA > 0, as illustrated in Figure 7. Again, the optimal catalyst is observed only if EA=0 and $G(H^+)$ = PA or pH = pK_a. If EA<0, the best "sub-optimal" catalyst happens for $G(H^+)$ = PA – EA/2, or pH = pK_a + EA/(2*2.303RT), with a thermodynamic overpotential of – EA/2F. If EA>0, the analysis predicts a flat-topped volcano with a flat top between $G(H^+)$ = PA – EA and $G(H^+)$ = PA + 2*EA with a thermodynamic overpotential of EA/F. In all cases, the analysis clearly predicts that the best catalyst operates with a pH close to the pK_a of the intermediate. This general statement is indeed used a design principle in the synthesis of molecular catalysts; for a recent example see ref.[59].

To demonstrate that the above conclusion is not an artifact of the thermodynamic analysis, the Appendix outlines a kinetic treatment of the model Eqs.19a-c, which yields the same result.

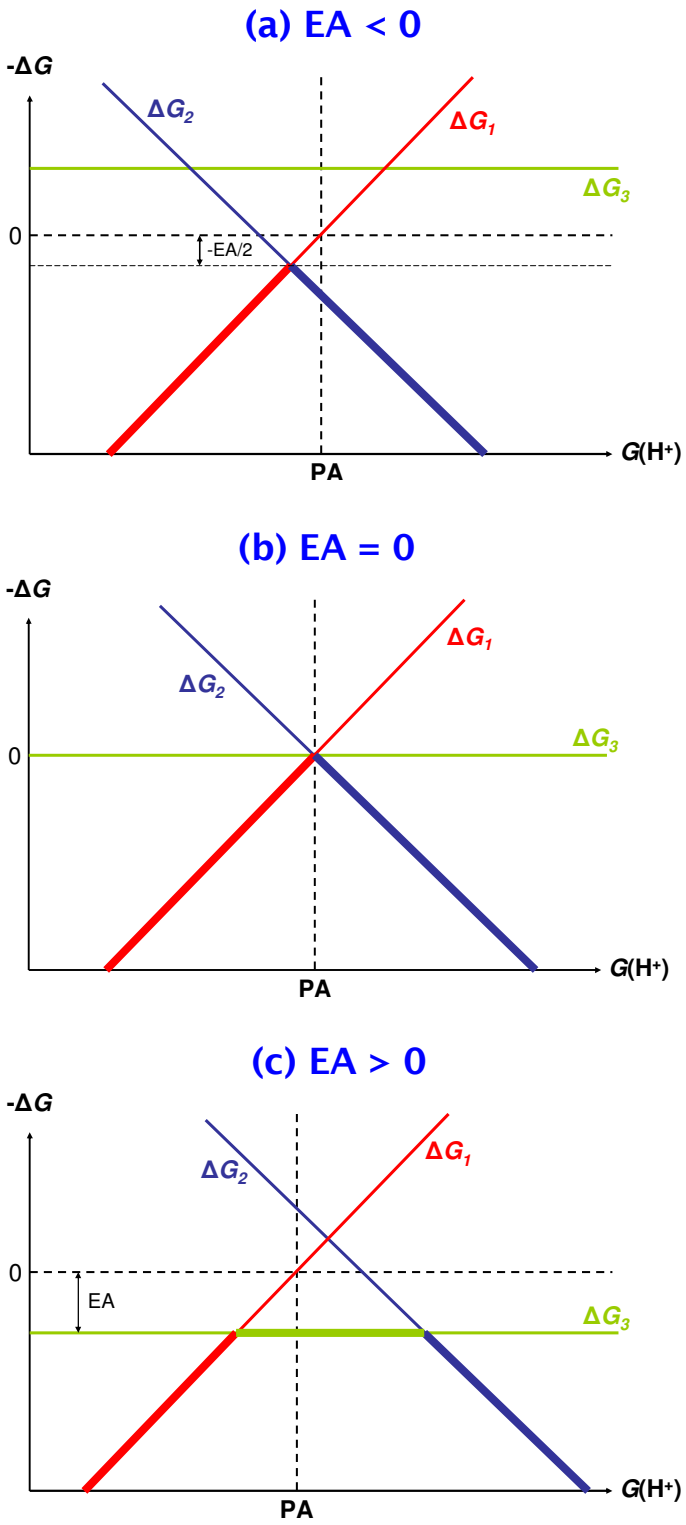

Figure 7. Thermodynamic volcano plots with $G(H^+)$ = -2.303RTpH as descriptor for the reaction mechanism represented by Eqs.17a, 17b and 17c. (a) EA< 0, (b) EA = 0, (c) EA > 0.

The same analysis can be applied to the blue-arrowed pathway in Figure 4,

$$A + e^- \leftrightarrows A^- \quad (24a)$$

$$A^- + H^+ + e^- \leftrightarrows AH^- \quad (24b)$$

$$AH^- + H^+ \leftrightarrows AH_2 \quad (24c)$$

as well as to the pathway indicated by the green arrows, in which the formation of the AH is not avoided but still involves a decoupled proton-coupled electron transfer reaction, for instance because of the high electron affinity of A:

$$A + e^- \leftrightarrows A^- \quad (25a)$$

$$A^- + H^+ \leftrightarrows AH \quad (25b)$$

$$AH + H^+ e^- \leftrightarrows AH_2 \quad (25c)$$

It is not difficult to verify that both mechanisms lead to exactly the same equations as for the analysis of Eqs.19a-c. The conclusion must therefore be that for two-proton two-electron transfer reactions in which in one of the PCET steps takes place through decoupled proton-electron transfer, the solution pH must be adjusted to achieve optimal catalytic activity. Moreover, the optimal catalyst is not the same at each pH. Eventually, one is searching for the optimal catalyst at the optimal pH.

4. Four proton-coupled electron transfer (4-PCET); application to the oxygen reduction reaction

Since most (catalytic) multi-electron transfer reactions involve an even number of electrons, we will consider here the situation of a four proton-electron transfer reaction. The more general conclusions of this section will also apply to reactions involving

another (even) number of protons and electrons. I will explicitly treat the most commonly considered four proton-electron transfer reaction in the electrocatalysis literature, namely the oxygen electrode:

$$O_2 + 4\ H^+ + 4\ e^- \leftrightarrows 2\ H_2O \tag{26}$$

and will first summarize the universal scaling issue referred to in the Introduction. Next I will include the possibility of decoupled proton-electron transfer, and demonstrate its relevance to experimental data.

Fully concerted pathway. One of the currently most commonly accepted mechanisms for the four-electron transfer reduction of oxygen on a platinum electrode is:

$$O_2 + H^+ + e^- \leftrightarrows OOH_{ads} \tag{27a}$$

$$OOH_{ads} \leftrightarrows O_{ads} + OH_{ads} \tag{27b}$$

$$O_{ads} + H^+ + e^- \leftrightarrows OH_{ads} \tag{27c}$$

$$OH_{ads} + H^+ + e^- \leftrightarrows H_2O \tag{27d}$$

The free energies of these four reactions are given by the equations:

$$\Delta G_{O_2/OOH_{ads}} = \Delta G_a = G(OOH_{ads}) - G(O_2) - G(H^+) + e_0 E \tag{28a}$$

$$\Delta G_{OOH_{ads}/O_{ads},OH_{ads}} = \Delta G_b = G(O_{ads}) + G(OH_{ads}) - G(OOH_{ads}) \tag{28b}$$

$$\Delta G_{O_{ads}/OH_{ads}} = \Delta G_c = G(OH_{ads}) - G(O_{ads}) - G(H^+) + e_0 E \tag{28c}$$

$$\Delta G_{OH_{ads}/H_2O} = \Delta G_d = G(H_2O) - G(OH_{ads}) - G(H^+) + e_0 E \tag{28d}$$

At the overall equilibrium potential $E = E^0_{O_2/H_2O}$ =1.23 V, the optimal catalyst requires all these free energies to be equal to zero. If we chose $G(O_2)$ = 4.92 eV and $G(H_2O)$ = 0 eV,

and redefine the potential according to Eq.17, we obtain the "ideal catalyst" as $G(\mathrm{OOH_{ads}})$ = 3x1.23 = 3.69 eV, $G(\mathrm{O_{ads}})$ = 2x1.23 = 2.46 eV and $G(\mathrm{OH_{ads}})$ = 1.23 eV.[19] Anderson has also expressed the condition of the "ideal catalyst" in terms of the binding energies of these three intermediates, but he chose different reference energies.[47,60,61] Importantly, it has been found computationally that on many different catalysts, the (binding) energies of O, OH and OOH are not independent, but are related to each other by so-called scaling relationships:[15]

$$G(\mathrm{OOH_{ads}}) = 0.5 \times G(\mathrm{O_{ads}}) + K_{\mathrm{OOH}} \tag{29a}$$

$$G(\mathrm{OH_{ads}}) = 0.5 \times G(\mathrm{O_{ads}}) + K_{\mathrm{OH}} \tag{29b}$$

These scaling relationships are the result of the principles of chemical bonding; the factor 0.5 in Eqs.29 expresses the idea that whereas O makes a double bond to the catalyst (i.e has two unpaired valence electrons), OH and OOH make a single bond to the catalyst (i.e. have one unpaired valence electron). The constant "offsets" K_{OOH} and K_{OH} depend on the family of catalysts to which the scaling relationships apply (i.e. metal surfaces, oxide surfaces, molecular catalysts), but the key discovery in refs.19 and 20 was that their difference, i.e. K_{OOH} - K_{OH}, is fixed:

$$\Delta G_{\mathrm{OH}}^{\mathrm{OOH}} = K_{\mathrm{OOH}} - K_{\mathrm{OH}} \approx 3.2 \pm 0.2 \text{ eV} \tag{30}$$

where we quote the number suggested by Rossmeisl et al.[20], who have referred to Eq.30 as "universal scaling". This difference is independent of the type of catalyst, and expresses the difference in energy between uncoordinated OOH and OH. In fact, the energy difference is very close to the energy difference between HO_2^- and OH^- in aqueous solution, which can be calculated from their known equilibrium potentials[62] from O_2 (-0.076 V and 0.401 V at pH=14, respectively) to be ca. 3.4 eV (which in fact suggests that both HO_2 and OH bind to the surface by accepting an electron, which is not surprising considering DFT calculations on this matter[63]). Based on Eqs.29 and 30, we can rewrite Eqs.28:

$$\Delta G_{\mathrm{O_2/OOH_{ads}}} = \Delta G_{\mathrm{a}} = 0.5\times G(\mathrm{O_{ads}}) + K_{\mathrm{OH}} + \Delta G_{\mathrm{OH}}^{\mathrm{OOH}} - 3.69\mathrm{eV} \quad (31a)$$

$$\Delta G_{\mathrm{OOH_{ads}/O_{ads},OH_{ads}}} = \Delta G_{\mathrm{b}} = G(\mathrm{O_{ads}}) - \Delta G_{\mathrm{OH}}^{\mathrm{OOH}} \quad (31b)$$

$$\Delta G_{\mathrm{O_{ads}/OH_{ads}}} = \Delta G_{\mathrm{c}} = -0.5\times G(\mathrm{O_{ads}}) + K_{\mathrm{OH}} + 1.23\mathrm{eV} \quad (31c)$$

$$\Delta G_{\mathrm{OH_{ads}/H_2O}} = \Delta G_{\mathrm{d}} = -0.5\times G(\mathrm{O_{ads}}) - K_{\mathrm{OH}} + 1.23\mathrm{eV} \quad (31d)$$

Note that this identifies the "ideal" value of $\Delta G_{\mathrm{OH}}^{\mathrm{OOH}}$ as 2.46 eV. Figure 8 plots these ΔG_i as a function of $G(\mathrm{O_{ads}})$ for the specific case of $K_{\mathrm{OH}} = 0$, illustrating that the value of $\Delta G_{\mathrm{OH}}^{\mathrm{OOH}}$ being unequal to 2.46 is what is keeping the optimal situation from being achievable. Figure 8 also illustrates that the minimum thermodynamic overpotential is:

$$\eta_{\mathrm{T}}^{\mathrm{min}} = \frac{1}{2e_0}\left(\Delta G_{\mathrm{OH}}^{\mathrm{OOH}} - 2.46\right) \quad (32)$$

regardless of the actual value of K_{OH}.

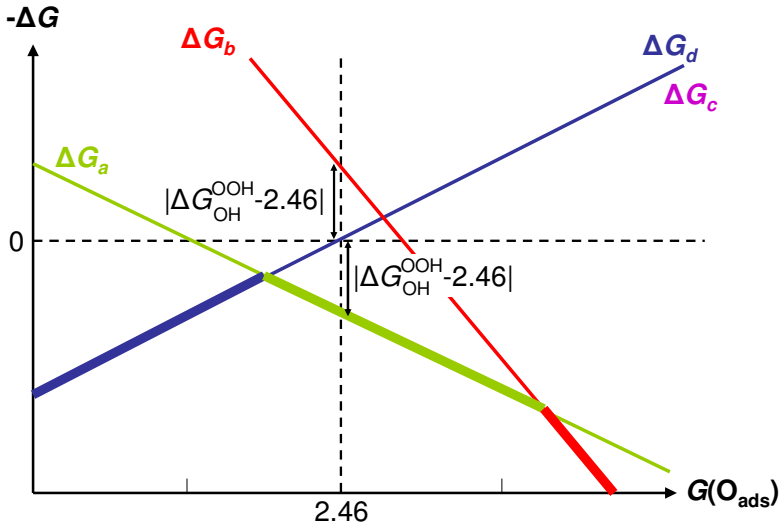

Figure 8. Thermodynamic volcano plot of Eqs.31a-d, representing reaction 27a-d, showing the influence of $\Delta G_{\mathrm{OH}}^{\mathrm{OOH}}$ in avoiding a completely reversible mechanism ($K_{\mathrm{OH}} = 0$ eV). If $\Delta G_{\mathrm{OH}}^{\mathrm{OOH}} = 2.46$ eV, all lines would intersect at $G(\mathrm{O_{ads}}) = 0$ eV and $\Delta G = 0$ eV.

Anderson and co-workers have recently suggested an equation similar to Eq.32.[47,60,61] Under conditions of the optimal catalyst in Fig.8, the only reaction in the mechanism that is exergonic is the dissociation of OOH_{ads}, reaction 27b. Anderson therefore explains the lack of reversibility in the ORR to the fact that the Gibbs free energy lost in the dissociation of OOH_{ads} is not available for electrical work, thereby leading to an "effective reversible potential" which has a value less than 1.23 V.[47,60] From Eqs.31 and Figure 8, it is straightforward to derive the following relation:

$$\eta_T = -\frac{1}{4e_0}\Delta G_{OOH_{ads}/O_{ads},OH_{ads}} \qquad (33)$$

which is Anderson's equation.[47,60] Importantly, we learn from Eq.31b that this recalcitrant exergonicity of reaction 27b is due to the high value of ΔG_{OH}^{OOH}. It is in principle possible to neutralize reaction 27b by a weak binding of O_{ads}, but in such a case the binding of OOH_{ads} will be so weak that reaction 27a is thermodynamically very unfavorable (see Figure 8). Therefore, I consider the unfavorable universal scaling between OOH and OH, i.e. the existence of ΔG_{OH}^{OOH} (Eq.30), to be a more fundamental reason for the "unavoidable" overpotential of the ORR and the OER (Eq.32), although for strong oxygen binding Anderson's interpretation (Eq.33) is essentially equivalent. For weak oxygen binding, when OOH_{ads} formation becomes potential determining, Anderson's equation is not applicable. However, under such conditions the mechanism represented by Eqs.27a-d may no longer be operative, as we will show in the next section.

Decoupled proton-electron pathways. The analysis in the previous section is valid for the mechanism given in Eqs.27, assuming the validity of the universal scaling relationship Eqs. 29 and 30. However, while the fact that the ORR polarization curve on polycrystalline and Pt(111) is essentially identical on the RHE scale irrespective of the pH (corresponding to a shift of 60 mV/pH on the NHE scale), suggests that on Pt indeed a concerted mechanism is followed,[64,65,66] it is well known that on other catalysts, the ORR does not follow the concerted proton-electron transfer mechanism implied by

Eqs.27. Mechanisms suggested for the ORR on enzymatic catalysts such as multi-copper enzymes or cytochrome c oxidase, never involve such concerted pathways.[25,67,68,69] In surface electrochemistry, catalysts that bind oxygen weakly, such as gold,[70,71] silver,[72] mercury,[73,74] and carbon[75] reduce oxygen in a de-coupled proton-electron transfer mechanism, although such electrodes often terminate the reduction reaction at the hydrogen peroxide stage (2 electron transfer mechanism). On these electrodes, the onset of the ORR does not shift with pH on the NHE scale, but shifts 60 mV/pH on the thermodynamically more relevant RHE scale. Below, we will analyze a mechanism for the ORR which explicitly accounts for a decoupled proton-electron transfer mechanism, and compare the predictions of this mechanism to some known experimental facts for the ORR on silver and gold electrodes.

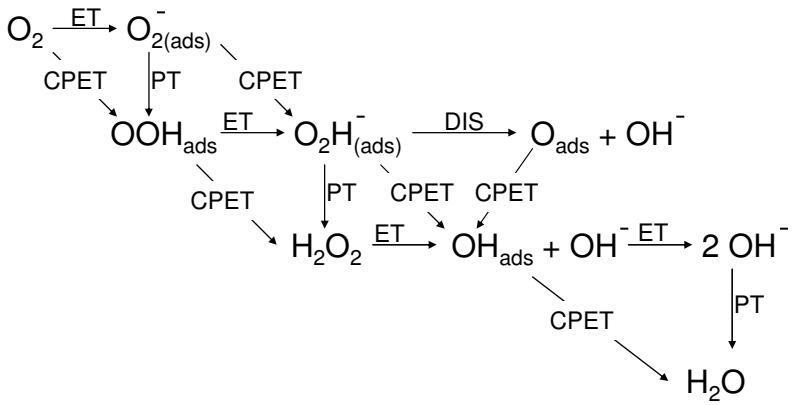

Figure 9. Mechanism considered for the oxygen reduction reaction on weakly adsorbing electrodes such as gold, silver and mercury.

The overall mechanism is shown in Figure 9. The mechanism drawn in Figure 9 does not consider the further reduction of H_2O_2 in acidic media, as neither gold, silver or mercury are able to reduce H_2O_2 in acidic media.[70,72,73] Let us first discuss the two-electron transfer mechanism to H_2O_2, for which Viswanathan et al.[76] have recently

considered a simple volcano on the basis on the fully concerted pathway via OOH_{ads}. From the analysis given in Section 3 on fully concerted two proton-transfer reactions, the binding energy of OOH for the optimal catalyst must be ca. 4.22 eV, as shown in Figure 10. However, in alkaline media, we must consider a competing decoupled proton-electron transfer pathway. In fact, on electrodes such as gold, mercury and carbon, it is well established that the rate-determining step in the ORR does *not* involve a proton. The first step is:

$$O_2 + e^- \rightarrow O^-_{2(ads)} \tag{34}$$

where (ads) indicates the species may or may not be (weakly) adsorbed. The standard equilibrium potential for this reaction is, on the Reversible Hydrogen Electrode (RHE) scale:[77]

$$E^{0,\mathrm{RHE}}_{O_2/O_2^-} / \mathrm{V} = -0.31 - \frac{\Delta G_{ads}(O_2^-)}{e_0} + 0.059 * pH \tag{35}$$

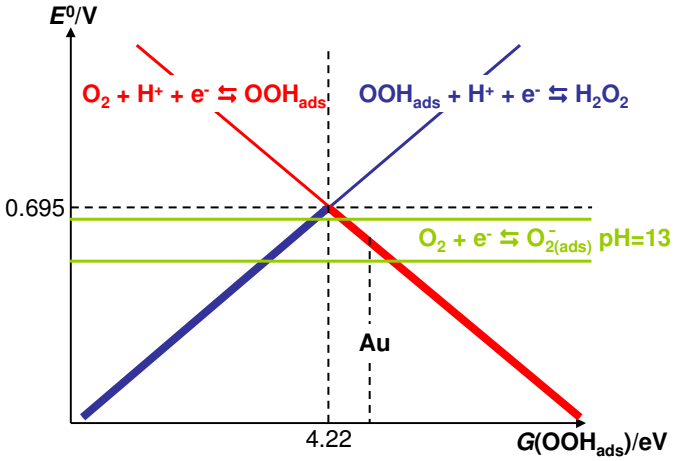

Figure 10. Thermodynamic volcano plot for the 2 electron-transfer reduction of oxygen to hydrogen peroxide, assuming an OOH_{ads} intermediate. On the strong (blue) binding leg, for binding energies lower than 4.22 eV, the concerted pathway is followed. On the weak (red) binding leg, for binding energies higher than 4.22 eV, the $O_2 + H^+ + e^- \leftrightarrows OOH_{ads}$ concerted pathway competes with the $O_2 + e^- \leftrightarrows O_2^-$ decoupled pathway, as indicated by the green lines for two values for the binding energy of $O^-_{2(ads)}$ (0 and -0.2 eV); at high pH, the latter pathway is thermodynamically more favorable.

We have drawn this potential in Figure 10 for a typical alkaline pH=13 and for zero and weak (-0.2 eV) Van der Waals-type binding of O_2^- to the surface. The standard equilibrium potential for OOH_{ads} formation calculated for Au(111)[76] is also indicated in Figure 10. As we discussed in Section 2, if the thermodynamic driving force for ET is comparable to that of CPET, ET tends to have the lower activation energy. Therefore, this analysis agrees with the experimental observation that in alkaline media the first step in the ORR on gold is reaction 34. As the pH is lowered, reaction 34 becomes thermodynamically less favorable, and the mechanism suggested by Viswanathan et al.[76] may become applicable. However, experimental measurements over a wide range of pH do not exhibit any pH dependence of the onset potential for ORR on Au on the SHE scale,[71] suggesting that reaction 34 is the first step of the ORR for all pH, and that OOH_{ads} is never formed in a concerted proton-transfer reaction (if at all). Hence, on a significant part of the "weak binding leg" of the volcano in Figure 10, a pathway different from the fully concerted pathway is followed. One of the further reasons why the concerted formation of OOH_{ads} could be disfavored if OOH binds weakly is that the solvent cross reorganization energy $\overline{\lambda}$ may be unfavorable, as in Figure 3C. The λ_{ET} for reaction 34 has been estimated from molecular dynamics simulations.[78] A similar model for the first step of the ORR on gold as a weakly interacting outer-sphere ET reaction was recently advocated by Quaino et al.[79]

The next step in the two-electron transfer mechanism could be either a PT or a CPET reaction (see Figure 9); we will exclude another ET step at this stage. The CPET reaction:

$$O_{2(ads)}^- + H_2O + e^- \rightarrow HO_{2(ads)}^- + OH^- \qquad (36)$$

has a standard equilibrium potential equal to:

$$E^0 = E^0_{O_2^-/HO_2^-} - \frac{\Delta G_{ads}(HO_2^-) - \Delta G_{ads}(O_2^-)}{e_0} \qquad (37)$$

with $E^0_{O_2^-/HO_2^-}$ = 0.413 V.[62] Clearly this is expected to be a favorable reaction at the relevant potential in alkaline media, and since OOH_{ads} is weakly bound, PT appears to be less likely. Costentin et al. also concluded reaction 36 to be a CPET reaction, albeit for water dissolved in an organic solvent.[80] Since the pK_a of H_2O_2 is 11.6, HO_2^- is the main product of the ORR on gold at pH=13. From the available experimental data, there does not appear to be an "optimal pH" for the ORR on gold, silver or mercury electrodes, suggesting that reaction 34 is the rate-determining step over the entire pH range.

Interestingly, Au(100) and silver electrodes (including Ag(111)) can perform the four-electron ORR, but only in alkaline media.[70,72,81,82] The exact reason for this has remained obscure. Especially the remarkable structure sensitivity of gold for the four-electron transfer has not yet been resolved, in spite of a number of DFT studies.[83,84] First of all, it should be mentioned that the unique ability of (100) surfaces to perform bond-breaking reactions under electrochemical conditions is quite common.[85] Such reactions often require well-defined two-dimensional (100) terraces, and the ORR on Au(100) is no exception, as steps in the Au(100) surface lower the selectivity for water.[70,82] Secondly, the pH dependence of the selectivity would suggest that HO_2^- is the precursor to the bond breaking reaction, as HO_2^- is indeed reduced to water only on Au(100).[86] Figure 9 suggests two pathways for bond breaking in HO_2^-. The first pathway labeled "DIS" is equivalent to reaction 27b as it does not involve proton or electron transfer (although OH^- is released, but without the involvement of water):

$$HO^-_{2(ads)} \rightarrow O_{ads} + OH^- \tag{38}$$

The second pathway is a CPET pathway:

$$HO^-_{2(ads)} + H_2O + e^- \rightarrow OH_{ads} + 2OH^- \tag{39}$$

The corresponding free energies are:

$$\Delta G_{HO_2^-/O_{ads},OH^-} = G(O_{ads}) - \Delta G^{OOH}_{OH} \tag{40}$$

where $\Delta G_{OH}^{OOH} \approx 3.4$ eV in this case, as mentioned earlier, and:

$$\Delta G_{HO_2^-/OH_{ads},OH^-} = G(OH_{ads}) - \Delta G_{OH}^{OOH} - G(H^+) + e_0 E \quad (41)$$

Since OH_{ads} binds considerably stronger to Au(100) than to Au(111), whereas the situation is exactly opposite for O_{ads}, and since HO_2 binds stronger to Au(100) than to Au(111) (as an anion),[84] we propose reaction 39 as the most likely O-O bond breaking reaction in the four-electron transfer ORR on Au(100) in alkaline media. We note that Strbac and Adzic have primarily focused on the role of chemisorbed OH on Au(100) in explaining its unique activity for the ORR.[70]

In the scheme of Figure 9, decoupling of proton and electron transfer happens because of the stabilization of species such as O_2^- and HO_2^- by their favorable electron affinity and their favorable interaction with the solution. Molecular catalysts and enzymes screen/neutralize such charged intermediates by changing oxidation state of the coordinating metal atom(s) instead of accompanying the electron transfer by concerted proton transfer. Since charge is too delocalized on a metal surface, this kind of charge screening is unlikely for surface electrochemistry, although it may be applicable to oxide surfaces which have a more localized charge character than metal surfaces. Eqs. 40 and 41 indicate that the involvement of HO_2^- would not really lift the issue of "universal scaling" for oxygen reduction, primarily because the value of ΔG_{OH}^{OOH} appears to be determined by the anionic binding character of OOH_{ads} (see above). An intermediate species often encountered in mechanisms of enzymatic dioxygen reduction is an unprotonated peroxo species O_2^{2-},[67,68,69] which is typically considered to be precursor to O-O bond breaking. Such a doubly decoupled proton-transfer mechanism would imply the existence of two intermediates with their own pK_a and therefore rather complicated pH dependence. A good example of such a mechanism from the recent literature is a paper by Cracknell and Blanford,[87] who studied the oxygen reduction reaction on a multicopper oxidase based on experiments using protein film voltammetry. In their model, the strong pH dependence of the oxygen reduction current is intimately related to the pK_a of (one of) the intermediate states. On the basis of the analysis of Section 3, it can

be predicted that in the case that two steps in the mechanism involve decoupled proton-electron transfer, these steps will have their own proper optimal pH. Therefore, their pK_as must not be too far apart for optimal catalysis.

5. Comparison to experiment

In the previous section, we showed how the experimental results of the ORR on "weakly adsorbing" electrodes should be viewed in terms of decoupled proton-electron transfer. This is not a new idea and the majority of the experimental surface electrochemistry literature on this subject has taken the same point-of-view. The general treatment suggested here is however applicable to any other reaction of the type given in Eq.1, and it is useful to discuss some recent experimental data in relation to the theoretical predictions.

Formic acid oxidation. The oxidation of formic acid on platinum electrodes is strongly pH dependent. A recent comprehensive experimental study showed that the oxidation activity peaks at pH ≈ 4.[88] Since the pK_a of formic acid is 3.75, this nicely confirms the general conclusion of Section 3. A kinetic model for formic acid oxidation, the essence of which is very similar to the model considered in the Appendix, confirmed the experimental observation. A non-electrochemical study of the pH-dependent formic acid decomposition by a molecular iridium-ruthenium complex also showed a peak in activity at pH ≈ 4.[89]

Alcohol oxidation. The electrochemical oxidation of alcohols on metal electrodes is very sensitive to pH, and is much more active in alkaline solution than in acidic solution. We have recently studied the oxidation of a series of similar poly-ols on a gold electrode and showed that the onset potential for oxidation scaled linearly with the pK_a of the corresponding alcohol.[90] Since the acidity of these alcohols is low (i.e. they have a high pK_a), alkaline media are preferred. This is consistent with a mechanism in which the deprotonation of the OH group of the alcohol precedes electron transfer, and this deprotonation takes place in solution, not at the electrode. It was also argued, in a subsequent paper,[91] that the second deprotonation step (from the C-H bond) needs a catalyst.

Carbon monoxide reduction. The reduction of carbon monoxide on a copper electrode is known to be strongly pH dependent. Hori et al.[92] have shown that this pH dependence is different for different products. The formation of methane is not pH dependent on the RHE scale, suggesting that the rate-determining step involves concerted proton-electron transfer. On the other hand, the formation of ethylene does not involve a proton, and is therefore not pH dependent on the SHE scale, but pH dependent of the RHE scale, and shifts closer to the overall equilibrium potential with increasing pH. According to the theory presented in Section 2, this implies that the first (rate-determining) step in the ethylene formation must involve an intermediate with a favorable electron affinity. In two recent papers,[93,94] we suggested that this intermediate could be an anionic CO dimer, which is indeed known to be a stable compound in the absence of water, known as acetylenediolate.[95] The fact that the ethylene formation takes place preferentially on a Cu(100) surface,[96] would suggest that this dimer has a favorable interaction with Cu(100).

6. Conclusions and perspectives

In this Perspective, a simple and general theoretical framework for multiple proton-electron transfer reactions has been outlined, based on the microscopic theory of proton-coupled electron transfer reactions, the thermodynamic theory of multi-step catalytic reactions, and the experimental realization that many multiple proton-coupled electron transfer reactions of the type given by Eq.1 feature decoupled proton-electron steps in their mechanism. The simple theory discussed for a two proton-electron transfer reaction shows that decoupling of proton and electron transfer leads to a pH dependence of the overall reaction rate, and a concomitant optimal pH for catalysis, which is close or equal to the pK_a of the key intermediate. This also implies a corresponding optimal catalyst at the optimal pH. In general, decoupled proton-electron transfer may occur if the reactant has a high electron or proton affinity for a reduction reaction, or a high tendency to give up a proton or an electron for an oxidation reaction. Comparison to experimental examples of decoupled proton-electron transfer in heterogeneous electrocatalysis (oxygen reduction, formic acid oxidation, alcohol oxidation, carbon monoxide reduction) suggest

that decoupled proton-electron transfer is more likely if the interaction of the intermediates with the catalyst is weak. Strong interaction between the electrode and the key intermediate, such as for the oxygen reduction reaction on platinum, tends to favor concerted proton-electron transfer; weak interaction between the electrode and the key intermediate leads to a more important role of the interaction with the solvent and the stabilization of "off-diagonal" intermediates, i.e. decoupled proton-electron transfer, such as for the oxygen reduction on gold. For oxidation reactions, such as alcohol oxidation and formic acid oxidation, deprotonation in solution plays a key role in the pH dependence of the reaction rate. The oxidation of alcohols prefers an alkaline pH, because of the high pK_a of the alcohol; the electro-oxidation of formic acid is optimal at a pH close its pK_a, as was recently confirmed experimentally,[88] in good agreement with theory prediction. It is expected that molecular catalysts and oxide catalysts are more likely to involve decoupled proton-electron transfer as they may screen charge locally by a change in oxidation state of a coordinating metal center. Such catalysts are therefore sensitive to pH.

A second important aspect of multiple proton-electron transfer reactions is the existence of scaling relations between the intermediates involved in the mechanism. In particular, two intermediates in a mechanism may bind to a catalyst in a similar manner (i.e. with the same valency) such that there is very little to no room to adjust the "universal" energy difference between them. As a result, there is a limit to how close one can come to a truly reversible catalyst, depending on how well the universal energy difference matches the thermodynamic requirement. Designing a three-dimensional active site to overcome such unfavorable energy differences seems to be the most direct strategy towards mitigating the negative consequences of universal scaling. However, the role of the solution side as part of this third dimension may also play a role, and pH could potentially be one of the parameters. It is therefore hoped that the present Perspective may help in formulating new strategies for designing better electrocatalysts.

Acknowledgements

I would like to thank Professor Masatoshi Osawa for his kind hospitality during my stay at Hokkaido University, and for useful discussions. I gratefully acknowledge the award of a Long-Term Fellowship of the Japanese Society for the Promotion of Science (JSPS), No. L-11527.

Appendix

In this Appendix, it is shown that the conclusion from the thermodynamic analysis in Section 3 of the paper also follows from a kinetic analysis, thus lending further credit to the main postulate on which the paper is based, namely that "*For optimal "reversible" electrocatalysis, the equilibrium potentials of all reaction steps must be equal to the overall equilibrium potential, or if non-electrochemical steps are involved, the Gibbs free energy of each reaction step must be zero*." For a possible mechanism for the hydrogen evolution, a similar analysis was performed in ref.48. Here, we will perform the analysis for the protonation mechanism 19a-c.

The overall reaction is:

$$A + 2H^+ + 2e^- \leftrightarrows AH_2 \qquad \text{(A1)}$$

with an equilibrium potential given by the Nernst equation:

$$E^{eq}_{A,\,2H^+/AH_2} = E^0_{A,\,2H^+/AH_2} + \frac{RT}{2F}\ln\left(\frac{c_A c^2_{H^+}}{c_{AH_2}}\right) \qquad \text{(A2)}$$

For a mechanism consisting of the following steps:

$$A + H^+ \leftrightarrows AH^+ \qquad \text{(reaction 1)}$$

$$AH^+ + H^+ + e^- \leftrightarrows AH_2^+ \qquad \text{(reaction 2)}$$

$AH_2^+ + e^- \leftrightarrows AH_2$ (reaction 3)

we write the following rate equations for the separate steps:

$$v_1 = k_1(c_A^0 - c_{AH^+})c_{H^+} - k_{-1}c_{AH^+} \tag{A3}$$

$$v_2 = k_2 c_{AH^+} c_{H^+} \exp\left(\frac{-\alpha_2 F(E-E_2^0)}{RT}\right) - k_{-2} c_{AH_2^+} \exp\left(\frac{(1-\alpha_2)F(E-E_2^0)}{RT}\right) \tag{A4}$$

$$v_3 = k_3 c_{AH_2^+} \exp\left(\frac{-\alpha_3 F(E-E_3^0)}{RT}\right) - k_{-3} c_{AH_2} \exp\left(\frac{(1-\alpha_3)F(E-E_3^0)}{RT}\right) \tag{A5}$$

Eqs.A3-A5 assume the Butler-Volmer kinetics[4] for the rates of reactions 2 and 3, with the α's the corresponding transfer coefficients. At the equilibrium potential, the rate of formation of AH_2 from reaction 3 is obtained by calculating the equilibrium concentration of AH_2^+ from Eq.A4 and the equilibrium concentration of AH^+ from Eq.A3, so that:

$$v_3^{\rightarrow} = k_3 \frac{c_A^0 c_{H^+}^2}{c_{H^+} + \frac{k_{-1}}{k_1}} \frac{k_2}{k_{-2}} \exp\left(\frac{-F(E-E_2^0)}{RT}\right) \exp\left(\frac{-\alpha_3 F(E-E_3^0)}{RT}\right) \tag{A6}$$

Note that this is also the measurable rate in case that reaction 3 is the rate-determining step. We want to evaluate this rate at the equilibrium potential of the overall reaction with $c_A = c_A^0$. If we set the activity of AH_2 equal to 1 for simplicity, and define corresponding equilibrium constants for reactions 1 and 2, we obtain:

$$v_3^{\rightarrow} = k_3 \frac{\left(c_A^0\right)^{1/2-\alpha_3/2} c_{H^+}^{1-\alpha_3}}{c_{H^+} + K_1^{-1}} K_2 \exp\left(\frac{-F\left((1+\alpha_3)E^0_{A,\,2H^+/AH_2} - E_2^0 - \alpha_3 E_3^0\right)}{RT}\right) \tag{A7}$$

The E^0's and K's in this equation are all constants, independent of pH. Figure A1 shows this rate as a function of pH, with all constants equal to unity and α_3 =0.5 and confirms that this plot is a volcano with a maximum at pH = exp[-2.303/K_1] = pK_a.

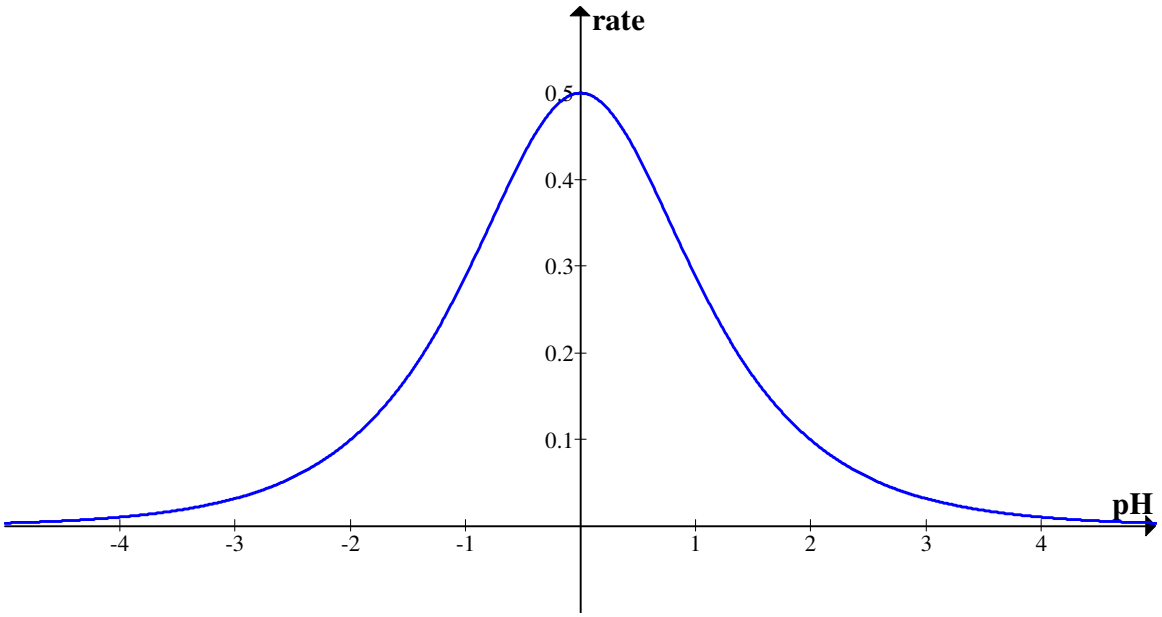

Figure A1. A plot of Eq.A7 for all constant equal unity and α_3 =0.5.

References

[1] M.T.M.Koper (Ed.), Fuel Cell Catalysis, A Surface Science Approach, Wiley & Sons (2008), Hoboken (NJ).
[2] D.Gust, T.A.Moore, A.L.Moore, Acc.Chem.Res. 2009, 42, 1890
[3] M.Rakowski Dubois, D.L.Dubois, Acc.Chem.Res. 2009, 42, 1974
[4] W.Schmickler, E.Santos, Interfacial Electrochemistry, Springer, 2nd Edition (2010), Heidelberg.
[5] R.A.Marcus, J.Chem.Phys. 1965, 43, 679
[6] P.Sabatier, Ber. Deutsch.Gem.Ges. 44 (1911) 1984
[7] J.A.Dumesic, G.W.Huber, M.Boudart, in Handbook of Heterogeneous Catalysis, 2nd ed., G.Ertl, H.Knözinger, F.Schüth, J.Weitkamp, Eds., Wiley-VCH, Wienheim (2008), p.1445
[8] J.K.Nørskov, T.Bligaard, J.Rossmeisl, C.H.Christensen, Nature Chem. 2009, 1 (2009) 37
[9] J.K.Nørskov, T.Bligaard, A.Logadottir, J.R.Kitchin, J.G.Chen, S.Pandelov, U.Stimming, J.Electrochem.Soc. 2005, 152, J23
[10] J.K.Nørskov, J.Rossmeisl, A.Logadottir, L.Lundqvist, J.R.Kitchin, T.Bligaard, H.Jónsson, J.Phys.Chem.B 2004, 108, 17886
[11] J.Rossmeisl, A.Logadottir, J.K.Nørskov, Chem.Phys. 2005, 319, 178
[12] J.Rossmeisl, Z.-W.Qu, H.Zhu, G.-J.Kroes, J.K.Nørskov, J.Electroanal.Chem. 2007, 607, 83
[13] A.Peterson, J.K.Nørskov, J.Phys.Chem.Lett. 2012, 3, 251
[14] P.Ferrin, A.U.Nilekar, J.Greeley, M.Mavrikakis, J.Rossmeisl, Surf.Sci. 2008, 602, 3424
[15] F.Abild-Petersen, J.Greeley, F.Studt, P.G.Moses, J.Rossmeisl, T.Munter, T.Bligaard, J.K. Nørskov, Phys.Rev.Lett. 2007, 99, 016105

[16] F.Calle-Vallejo, J.I. Martinez, J.M. Garcia-Lastra, J.Rossmeisl, M.T.M.Koper, Phys.Rev.Lett. 2012, 108, 116103
[17] E.Shustorovich, Surf.Sci.Rep. 1986, 6, 1
[18] F.Calle-Vallejo, N.G.Inoglu, H.-Y.Su, J.I.Martinez, I.C.Man, M.T.M.Koper, J.R.Kitchin, J.Rossmeisl, Chem.Sci. 2013, 4, **DOI:** 10.1039/C2SC21601A
[19] M.T.M.Koper, J.Electroanal.Chem. 2011, 660, 254
[20] I.C. Man, H.-Y.Su, F.Calle-Vallejo, H.A.Hansen, J.I.Martinez, N.G.Inoglu, J.R.Kitchin, T.F.Jaramillo, J.K.Nørskov, J.Rossmeisl, ChemCatChem 2011, 3, 1159
[21] F.Calle-Vallejo, J.I.Martinez, J.Rossmeisl, Phys.Chem.Chem.Phys. 2011, 13, 15639
[22] F.Calle-Vallejo, J.I. Martinez, J.M. Garcia-Lastra, E. Abad, M.T.M.Koper, Surf.Sci. 2013, 607, 47
[23] V.Viswanathan, H.A.Hansen, J.Rossmeisl, J.K.Nørskov, ACS Catal. 2012, 2, 1654
[24] H.A.Hansen, J.B.Varley, A.Peterson, J.K.Nørskov, J.Phys.Chem.Lett. 2013, 4, 388
[25] M.T.M.Koper, H.A.Heering, in "Fuel Cell Science: Theory, Fundamentals, and Bio-Catalysis", A.Wieckowski, J.K.Nørskov (Eds.), Wiley-VCH, New York, 2010, p.71.
[26] R.I.Cukier, D.G.Nocera, Annu.Rev.Phys.Chem. 1998, 49, 337
[27] A.V.Soudackov, S.Hammes-Schiffer, J.Chem.Phys. 1999, 111, 4672
[28] A.M.Kuznetsov, J.Ulstrup, Rus.J.Electrochem. 2003, 39, 9
[29] J.Grimminger, S.Bartenschlager, W.Schmickler, Chem.Phys.Lett. 2005, 416, 316
[30] C.Costentin, M.Robert, J-M.Savéant, J.Electroanal.Chem. 2006, 588, 197
[31] C.Costentin, M.Robert, J-M.Savéant, Acc.Chem.Res. 2010, 43, 1019
[32] S.Hammes-Schiffer, A.A.Stuchebrukhov, Chem.Rev. 2010, 110, 6939
[33] M.T.M.Koper, Phys.Chem.Chem.Phys. 2013, 15, 1399
[34] C.Hartnig, M.T.M.Koper, J.Chem.Phys. 2001, 115, 8540
[35] L.Onsager, J.Am.Chem.Soc. 1936, 58, 486
[36] J.G.Kirkwood, J.Chem.Phys. 1939, 7, 911
[37] A.Weller, Prog. React.Kinet. 1961, 1, 187
[38] M.Eigen, Angew.Chem.Int.Ed. 1964, 3, 1
[39] S.Hammes-Schiffer, ChemPhysChem 2002, 3, 33
[40] A.V.Soudackov, A.Hazra, S.Hammes-Schiffer, J.Chem.Phys. 2011, 135, 144115
[41] B.Auer, A.V.Soudackov, S.Hammes-Schiffer, J.Phys.Chem.C 2012, 116, 7695
[42] N.Iordanova, S.Hammes-Schiffer, J.Am.Chem.Soc. 2001, 124, 4848
[43] E.Hatcher, A.V.Soudackov, S.Hammer-Schiffer, J.Am.Chem.Soc. 2004, 126, 5673
[44] S.Hammes-Schiffer, A.V.Soudackov, J.Phys.Chem.B 2008, 112, 14108
[45] C.Costentin, M.Robert, J.-M.Savéant, J.Am.Chem.Soc. 2007, 129, 5870
[46] E.Santos, M.T.M.Koper, W.Schmickler, Chem.Phys. 2008, 344, 195
[47] A.B.Anderson, Phys.Chem.Chem.Phys. 2012, 14, 1330
[48] M.T.M.Koper, J.Solid State Electrochem. 2013, 17, 339
[49] J.A.Dumesic, J.Catal. 1999, 185, 496
[50] C.T.Campbell, J.Catal. 2001, 204, 520
[51] J.A.Dumesic, J.Catal. 2001, 204, 525
[52] C.Stegelmann, A.Andreasen, C.T.Campbell, J.Am.Chem.Soc. 2009, 131, 8077
[53] R.Parsons, Trans.Faraday Soc. 1958, 34, 1053
[54] R.Parsons, in Catalysis in Electrochemistry: From Fundamental Aspects to Strategies for Fuel Cell Development, E.Santos, W.Schmickler (Eds.), Wiley-VCH, Hoboken NJ, USA (2011) p.1
[55] H.Gerischer, Bull.Soc.Chim.Belg. 1958, 67, 506
[56] B.Hinneman, P.G.Moses, J.Bonde, K.P.Jørgensen, J.H.Nielsen, S.Horch, I.Chorkendorff, J.K. Nørskov, J.Am.Chem.Soc. 2005, 127, 5308
[57] M.T.M.Koper, H.A.Heering, in "Fuel Cell Science: Theory, Fundamentals, and Bio-Catalysis", A.Wieckowski, J.K.Nørskov (Eds.), Wiley-VCH, New York, 2010, p.71.
[58] J.Greeley, J.K.Nørskov, L.A.Kibler, A.M.El-Aziz, D.M.Kolb, ChemPhysChem 2006, 7, 1032
[59] Y.A.Small, D.L.DuBois, E.Fujita, J.T.Muckerman, Energy Environ.Sci. 2011, 4, 3008
[60] F.Tian, A.B.Anderson, J.Phys.Chem.C 2011, 115, 4076
[61] A.B.Anderson, R.Jinnouchi, J.Uddin, J.Phys.Chem.C 2013, 117, 41
[62] A.J.Bard, R.Parsons, J.Jordan (Eds.), Standard Potentials in Aqueous Solution, Marcel Dekker Inc., New York, 1985

[63] A.Panchenko, M.T.M.Koper, T.E.Shubina, S.J.Mitchell, E.Roduner, J.Electrochem.Soc. 2004, 151, A2016
[64] M.R. Tarasevich, A.Sadkowski, E. Yeager, in: B.E. Conway, J.O.M Bockris, E. Yeager, S.U.M. Khan, R.E. White (Eds.), Comprehensive Treatise of Electrochemistry, Vol.7, Plenum Press, New York, 1983, pp. 301–398.
[65] N.M.Markovic, P.N.Ross, Surf.Sci.Reports 2002, 45, 117
[66] M.F.Li, L.W.Liao, D.F.Yuan, D.Mei, Y.-X.Chen, S.Ye, to be published; Y-.X.Chen, M.F.Li, L.W.Liao, D.F.Yuan, Y.L.Zheng, abstract presented at the 63rd Annual Meeting of the International Society of Electrochemistry.
[67] E.I.Solomon, P.Chen, M.Metz, S.-K.Lee, A.E.Palmer, Angew.Chem.Int.Ed. 2001, 40, 4570
[68] E. I. Solomon, A. J. Augustine, and J. Yoon, Dalton Trans. 2008, 3921
[69] J.A.Fee, D.A.Case, L.Noodleman, J.Am.Chem.Soc. 2008, 130, 15002
[70] S.Strbac, R.R.Adzic, Electrochim.Acta 1996, 41, 2903
[71] Q.J.Chen, Y.L.Zheng, L.W.Liao, J.Kang, Y.-X.Chen, Scientia Sinica Chimica 2011, 41, 1777
[72] B.B.Blizanac, P.N.Ross, N.M.Markovic, Electrochim.Acta 2007, 52, 2264
[73] C.J.van Velzen, M.Sluyters-Rehbach, A.G.Remeijnse, G.J.Brug, J.H.Sluyters, J.Electroanal.Chem. 1982, 134, 87
[74] C.J.van Velzen, A.G.Remeijnse, M.Sluyters-Rehbach, J.H.Sluyters, J.Electroanal.Chem. 1982, 142, 229
[75] H.-H.Yang, R.L.McCreery, J.Electrochem.Soc. 2000, 147, 3420
[76] V.Viswanathan, H.A.Hansen, J.Rossmeisl, J.K.Nørskov, J.Phys.Chem.Lett. 2012, 3, 2948
[77] J.Xu, W.Huang, R.L.McCreery, J.Electroanal.Chem. 1996, 410, 235
[78] C.Hartnig, M.T.M.Koper, J.Electroanal.Chem. 2002, 532, 165
[79] P.Quaino, N.Luque, R.R.Nazmutdinov, E.Santos, W.Schmickler, Angew.Chem.Int.Ed. 2012, 51, 12997
[80] C.Costentin, D.H.Evans, M.Robert, J.-M.Savéant, P.S.Singh, J.Am.Chem.Soc. 2005, 127, 12490
[81] N.M.Markovic, R.R.Adzic, V.B.Vesovic, J.Electroanal.Chem. 1984, 165, 105
[82] S.Strbac, R.R.Adzic, J.Electroanal.Chem. 1996, 403, 169
[83] J.Kim, A.A.Gewirth, J.Phys.Chem.B 2006, 110, 2565
[84] P.Vassilev, M.T.M.Koper, J.Phys.Chem.C 2007, 111, 2607
[85] M.T.M.Koper, Nanoscale 2011, 3, 2052
[86] S.Strbac, R.R.Adzic, J.Electroanal.Chem. 1992, 337, 355
[87] J.A.Cracknell, C.F.Blanford, Chem.Sci. 2012, 3, 1567
[88] J.Joo, T.Uchida, A.Cuesta, M.T.M.Koper, M.Osawa, to be submitted
[89] S.Fukuzumi, T.Kobayashi, T.Suenobu, J.Am.Chem.Soc. 2010, 132, 1496
[90] Y.Kwon, S.C.S.Lai, P.Rodriguez, M.T.M.Koper, J.Am.Chem.Soc. 2011, 133, 6914
[91] P.Rodriguez, Y.Kwon, M.T.M.Koper, Nature Chem. 2012, 4, 177
[92] Y.Hori, I.Takahashi, O.Koga, N. Hoshi, J.Phys.Chem.B 2002, 106, 15
[93] K.J.P.Schouten, Y.Kwon, C.J.M.van der Ham, Z.Qin, M.T.M.Koper, Chem.Sci. 2011, 2, 1902
[94] F.Calle-Vallejo, M.T.M.Koper, submitted for publication
[95] E.Weiss, W.Büchner, Helv. Chim. Acta 1963, 46, 1121.
[96] K.J.P.Schouten, Z.Qin, E.Perez Gallent, M.T.M.Koper, J.Am.Chem.Soc. 2012, 134, 9864